Clim. Past Discuss., https://doi.org/10.5194/cp-2019-10
Manuscript under review for journal Clim. Past
Discussion started: 11 February 2019

Climate of the Past Discussions
Open Access
EGU

How large are temporal representativeness errors in paleoclimatology?

Daniel E. Amrhein[1]

[1]University of Washington School of Oceanography and Department of Atmospheric Sciences

Correspondence: Dan Amrhein (amrhein@uw.edu)

Abstract. Ongoing work in paleoclimate reconstruction prioritizes understanding the origins and magnitudes of errors that arise when comparing models and data. One class of such errors arises from assumptions of proxy temporal representativeness – broadly, the time scales over which paleoclimate proxy measurements are associated with climate variables. In the case of estimating time mean values over an interval, errors can arise when the time interval over which data are averaged and the interval that is being studied have different lengths, or if those intervals are offset from one another in time. Because it is challenging to tailor proxy measurements to precise time intervals, such errors are expected to be common in model-data and data-data comparisons, but how large and prevalent they are is unclear. The goal of this work is to provide a framework for first-order quantification of temporal representativity errors and to study the interacting effects of sampling error, archive smoothing (e.g. by bioturbation in sediment cores), chronological offsets and errors (e.g. arising from radiocarbon dating), and the spectral character of the climate process being sampled.

In some cases, particularly for small values of target intervals τ_x relative to sample intervals τ_y, errors can be large relative to signals of interest. Errors from mismatches in τ_x and τ_y can have magnitudes comparable to those from chronological uncertainty. Archive smoothing can reduce sampling errors by acting as an anti-aliasing filter, but destroys high-frequency climate information. An extension of the approach to paleoclimate time series, which are sequences of time-average values, shows that measurement intervals shorter than the spacing between samples lead to errors, absent compensating effects from archive smoothing. Including these sources of uncertainty will improve accuracy in model-data comparisons and data comparisons and syntheses. Moreover, because sampling procedures emerge as important parameters in uncertainty quantification, reporting salient information about how records are processed and assessments of archive smoothing and chronological uncertainties alongside published data is important to be able to use records to their maximum potential in paleoclimate reconstruction and data assimilation.

1 Introduction

Paleoclimate records provide important information about the variability, extremes, and sensitivity of Earth's climate to greenhouse gases on time scales longer than the instrumental period. As the number of published paleoclimate records has grown and the sophistication of numerical model representations of past climates has improved, it has become increasingly important to understand the uncertainty with which paleoclimate observations represent climate variables so that they can be compared

Clim. Past Discuss., https://doi.org/10.5194/cp-2019-10
Manuscript under review for journal Clim. Past
Discussion started: 11 February 2019

to one another and to model output. Additionally, quantifying uncertainty is important for ongoing efforts to assimilate paleoclimate data with numerical climate models (e.g., Hakim et al., 2016; Amrhein et al., 2018).

Paleoclimate records can have errors arising from many different sources: biological effects (e.g., Elderfield et al., 2002; Adkins et al., 2003), aliasing onto seasonal cycles (Wunsch, 2000; Fairchild et al., 2006; Dolman and Laepple, 2018), spatial representativeness (Van Sebille et al., 2015), proxy-climate calibrations (e.g., Tierney and Tingley, 2014), and instrument errors, to name a few. This paper focuses on errors from temporal representativeness (TR), which we define as the degree to which a measurement averaging over one time interval can be used to represent a second, target time interval. In this paper we quantify TR errors arising 1) when averages are computed over different lengths of time and 2) when intervals are offset so as to be centered on different times (Figure 1). For instance, in a data assimilation procedure that fits a model to observations at every year, it is important to know the uncertainty associated with relating a decadal-average proxy observation to an annual-average target interval. Furthermore, computing a mean is often the implicit goal of binning procedures that combine observations from within a target time period such as a marine isotope stage, and we expect those observations to have errors that vary with their averaging duration and offsets from the target. TR errors can result both from systematic errors (e.g., knowingly using data from a short period to represent a longer one) and from stochastic uncertainties in the duration and age of paleoclimate observations that can originate, e.g., from uncertain radiocarbon age measurements.

Much of the previous study of errors arising from sampling in time has focused on aliasing, whereby variability at one frequency in a climate process appears at a different frequency in discrete samples of that process. Pisias and Mix (1988) described consequences of aliasing in the study of deterministic peaks in climate spectra due to Milankovich forcing. Wunsch and Gunn (2003) described criteria for choosing sample spacing so as not to alias low-frequency variability in sediment cores, and Wunsch (2000) demonstrated how aliasing can lead to spurious spectral peaks in ice core records. Beer et al. (2012) and von Albedyll et al. (2017) describe how running means can reduce aliasing of solar cycle variability in ice core records. In paleoclimate, measurements are often unevenly spaced in time due to changes in archive deposition rates; Jones (1972) showed that aliasing is present and even exacerbated in unevenly-sampled records relative to regularly sampled ones. Anderson (2001) and McGee et al. (2013) describe how bioturbation and other diagenetic processes smooth records in time and may reduce aliasing errors.

A second area of previous focus stems from chronological uncertainties, whereby times assigned to measurements may be biased or uncertain. In some cases, such as for radiocarbon dating, estimates of these uncertainties are available from Bayesian approaches that incorporate sampling procedures (Buck, 2004; Buck and Millard, 2004; Bronk Ramsey, 2009); practices for incorporating this information into model-data or data-data comparisons vary, and developing tools for analyzing chronological uncertainty is an active area of research. Huybers and Wunsch (2004) include the effect of uncertainties in tie points in order to align multiple records of Pleistocene oxygen isotopes, and Haam and Huybers (2010) developed tools for estimating the statistics of time-uncertain series. The effect of time uncertainty on estimates of signal spectra is modest in some cases (Rhines and Huybers, 2011), in part because time uncertainty acts to smooth high-frequency variability when computed as an expectation over a record (Moore and Thomson, 1991).

Clim. Past Discuss., https://doi.org/10.5194/cp-2019-10
Manuscript under review for journal Clim. Past
Discussion started: 11 February 2019

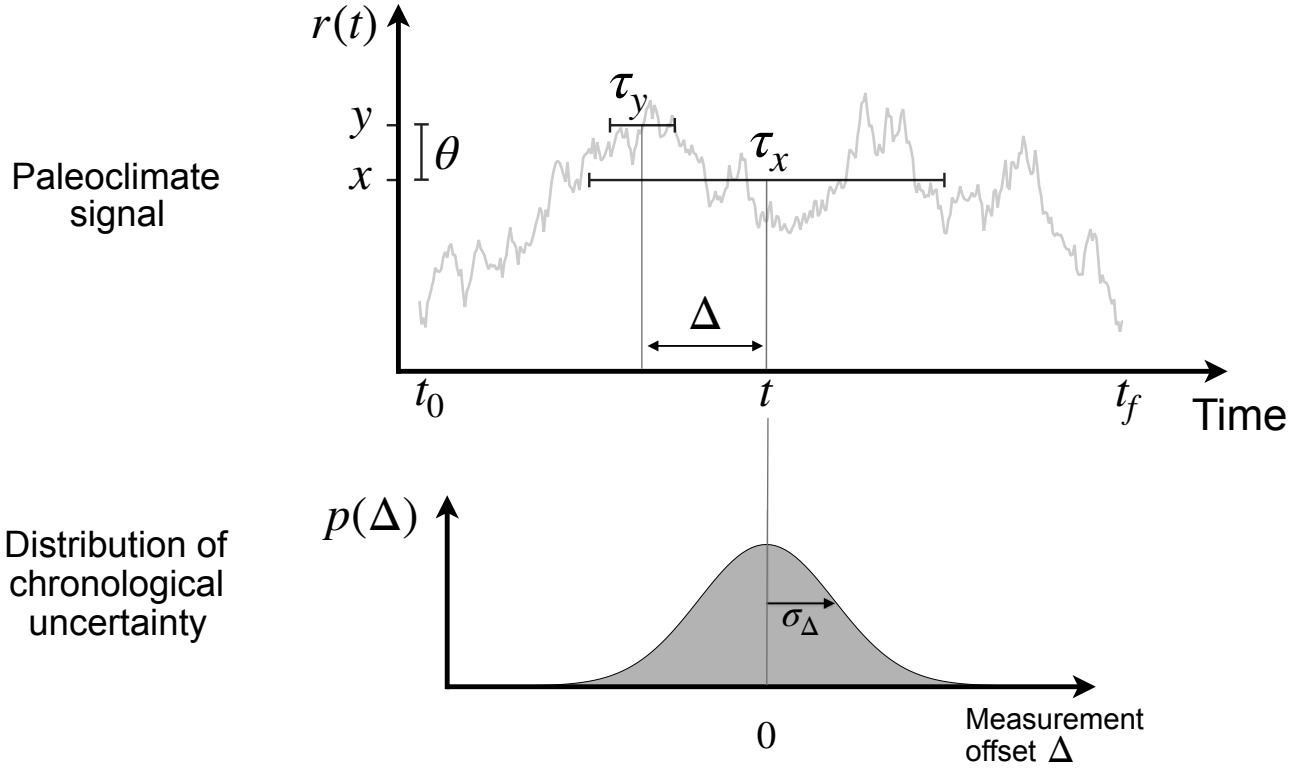

Figure 1. Schematic of temporal representativeness errors. When a target time-average quantity (x) of a paleoclimate signal ($r(t)$) is estimated using an observation (y), an error (θ) results if the averaging interval of the observation (τ_y) is different from that of the target period (τ_x), including a nonzero offset (Δ) between the centers of the two time averages. When a measurement is affected by chronological uncertainty, Δ is characterized by a probability distribution ($p(\Delta)$) of possible offsets, parameterized in this paper as a Gaussian with standard deviation σ_Δ. This paper characterizes the amplitude of θ as a function of time scales arising from 1) sampling procedures, 2) variability in $r(t)$, 3) archive smoothing, and 4) chronological uncertainty.

Clim. Past Discuss., https://doi.org/10.5194/cp-2019-10
Manuscript under review for journal Clim. Past
Discussion started: 11 February 2019

Climate of the Past Discussions

This paper synthesizes effects contributing to TR errors in an analytical model and explores their amplitudes and dependence on signal spectra and sampling time scales. Extending results from time-mean measurements to time series demonstrates how sampling practices can lead to aliasing errors when records are not sampled densely, e.g. when an ocean sediment core is not sampled continuously along its accumulation axis. While we do not claim that TR error is the most important source of uncertainty in paleoclimate records, it does appear to be large enough to affect results in some cases. Moreover, this work is a step towards reducing the number of "unknown unknowns" in paleoclimate reconstruction.

The rest of the paper is as follows. Section 2 describes a statistical model for time representativeness errors in time mean values. Section 3 illustrates the model by applying it to the analysis of Last Glacial Maximum climate properties. Section 4 extends the model to the analysis of time series. Implications, caveats, and future research questions appear in the Discussion. Table (1) provides a glossary of functions and variables used.

2 A statistical model for temporal representativeness errors

In paleoclimatology, a common focus is computing the mean of a climate variable (sea surface temperature, for instance, or isotope ratios, or global ice volume) over a particular time period (for example, a marine isotope stage). This section defines an analytical approach for estimating temporal representativity errors in the problem of mean estimation. These errors have a compact representation in the frequency domain that allows us to understand the relative importance and interaction of sampling procedures, time uncertainty, and signal spectra in contributing to errors.

This approach is intended to be complementary to the output from proxy system models (PSMs; e.g., Evans et al. (2013)) that relate proxy quantities to climate variables. The analytical model may be used to estimate TR uncertainty when PSMs do not; when they do, the model can provide a theoretical grounding for understanding those results. The starting point for the model is a climate process, $r(t)$, which we assume to be able to sample directly. We ignore additional errors that are inherited from the construction of $r(t)$ from proxy observations. Variances from multiple error sources can be added together under the approximations that they are independent and Gaussian. When these assumptions fail, more holistic forward modeling of errors in PSMs may be necessary.

2.1 Errors in time-mean values

Define a mean value $m(t,\tau)$ of a climate variable $r(t)$ as a function of the duration τ and the time t on which that duration is centered,

$$m(t,\tau) = \int_{-\infty}^{\infty} \Pi(t',\tau)\, r(t+t')\, dt', \tag{1}$$

Clim. Past Discuss., https://doi.org/10.5194/cp-2019-10
Manuscript under review for journal Clim. Past
Discussion started: 11 February 2019

Climate of the Past Discussions
Open Access
EGU

Variable	Meaning
t	Time
t_0	Initial time in a time series
t_f	Final time in a time series
ν	Frequency
ν_{Nyq}	Nyquist frequency
$\nu^{\dagger}_{low}$	Lower cutoff frequency
$\nu^{\dagger}_{high}$	Upper cutoff frequency
$r(t)$	Time-varying climate process
$m(t,\tau)$	Time mean of $r(t)$ over period τ centered on t
x	Target paleoclimate quantity
y	Measured paleoclimate quantity
θ	Error in representing x by y
τ_x	Averaging timescale of target quantity
τ_y	Averaging timescale of observation
τ_a	Timescale of archive smoothing
τ_s	Time interval between samples in a series
τ_0	Time series length (equal to $t_f - t_0$)
τ_c	Time between two time means being compared
Δ	Measurement time offset
σ_Δ	Standard deviation of chronological error
σ_{τ_c}	Expected difference between two time means separated by τ_c
$\Pi(t,\tau)$	Boxcar function in time
$G(\nu,\tau)$	Heaviside function in frequency
$H(\nu)$	Power transfer function
f	Error variance fraction
β	Spectral slope (times -1)

Table 1. Glossary of functions and variables. Variables denoted by a superscript i in the text denote the i^{th} value of that quantity in a time series. Fourier transformed variables are denoted by a hat (e.g., $\hat{r}(\nu)$).

Clim. Past Discuss., https://doi.org/10.5194/cp-2019-10
Manuscript under review for journal Clim. Past
Discussion started: 11 February 2019

Climate of the Past Discussions

where $\Pi(t,\tau)$ is a normalized "boxcar" function centered on $t=0$ with width τ,

$$\Pi(t,\tau) = \begin{cases} 1/\tau & |t| \le \tau/2 \\ 0 & |t| > \tau/2. \end{cases} \tag{2}$$

The operation in (1) defines a moving average $m(t,\tau)$ and is known as a convolution, hereafter denoted as a star,

$$m(t,\tau) = \Pi(t,\tau) \star r(t). \tag{3}$$

Our focus is on errors that arise when a mean value computed over one time period is used to represent another time period – for instance, when a time average over over 20-19 kya (thousand years ago) is used to represent an average over 23-19 kya, the nominal timing of the Last Glacial Maximum (Clark et al., 2012). To write this representation generally, define a target quantity to be a mean x of $r(t)$ over an interval of length τ_x centered on t, and an observation y to be an average over a different duration τ_y centered on a different time $t+\Delta$,

$$x = m(t,\tau_x) \tag{4}$$

$$y = m(t+\Delta,\tau_y). \tag{5}$$

(While these quantities are functions of several variables, we write them simply as x and y for brevity.) In many cases, paleoclimate archive are smoothed prior to processing by bioturbation, diagenesis, residence times in karst systems upstream of speleothems (Fairchild et al., 2006), or other effects. These processes can be complex and non-constant in time; here, to gain a basic understanding of their effects, we assume an archive smoothing process that is a moving average over a time scale τ_a. Under such smoothing, we can then write y as a twice-smoothed function of $r(t)$,

$$y = \Pi(t,\tau_y) \star \Pi(t,\tau_a) \star r(t).$$

TR error is defined as the error in representing x by y,

$$\theta = x - y. \tag{6}$$

We will characterize TR error θ by estimating its variance, $\left\langle (\theta - \langle\theta\rangle)^2 \right\rangle$, where angle brackets denote statistical expectation. This approach assumes that $r(t)$ is weakly statistically stationary, meaning that its mean and variance do not change in time; caveats surrounding this assumption are addressed later in the paper. Under the weak stationarity assumption, the mean error $\langle\theta\rangle$ is zero, and we take the expectation by evaluating θ^2 at all the times in $r(t)$ to compute the variance,

$$\left\langle \theta^2 \right\rangle = \frac{1}{\tau_0} \int_{t_0}^{t_f} (x-y)^2 dt, \tag{7}$$

where t_0 and t_f are the initial and final times in $r(t)$, and $\tau_0 = t_f - t_0$. Intuitively, we are estimating the error in representing x by y *(at a single time)* as the time-mean squared difference of running means of $r(t)$. In practice, though we do not know $r(t)$, knowledge of its statistics is adequate to estimate $\left\langle \theta^2 \right\rangle$. To show this, define $x' = x - \langle x\rangle$ and $y' = y - \langle y\rangle$, where $\langle x\rangle = \langle y\rangle$ for

Clim. Past Discuss., https://doi.org/10.5194/cp-2019-10
Manuscript under review for journal Clim. Past
Discussion started: 11 February 2019

Climate of the Past Discussions

stationary $r(t)$. Then expanding (7) gives an expression in terms of estimated variances $\tilde{\sigma}_x^2$ and $\tilde{\sigma}_y^2$ and the cross-covariance as a function of lag Δ, $\tilde{C}_{xy}(\Delta)$:

$$\left\langle \theta^2 \right\rangle = \frac{1}{\tau_0} \int_{t_0}^{t_f} \left(x' - y'\right)^2 dt \tag{8}$$

$$= \frac{1}{\tau_0} \left(\int_{t_0}^{t_f} x'^2 dt + \int_{t_0}^{t_f} y'^2 dt - 2 \int_{t_0}^{t_f} x' y' \, dt \right) \tag{9}$$

$$= \tilde{\sigma}_x^2 + \tilde{\sigma}_y^2 - 2\tilde{C}_{xy}(\Delta). \tag{10}$$

In the limit where $\tau_x = \tau_y$ and $\Delta = 0$, $\tilde{\sigma}_x^2 = \tilde{\sigma}_y^2 = \tilde{C}_{xy}(\Delta)$, and $\left\langle \theta^2 \right\rangle = 0$, as we would expect for the case where the measurement exactly targets the quantity of interest. If $\tilde{C}_{xy}(\Delta) = 0$ – i.e., the measurement and target quantity are uncorrelated – then y has no skill in representing x, and the error variance is the sum of $\tilde{\sigma}_x^2$ and $\tilde{\sigma}_y^2$. If there is a choice of Δ such that x and y are anticorrelated, then $\tilde{C}_{xy}(\Delta)$ will be negative, leading to still larger errors. Between these extremes of zero and maximum error, intermediate values of $\left\langle \theta^2 \right\rangle$ are set by timescales of sampling (τ_x, τ_y, and Δ) and variability in $r(t)$. We can understand these relationships by representing TR error in the frequency domain.

2.2 Analyzing sources of error in the frequency domain

Next we derive a frequency-domain expression for TR errors. The functional form of this expression provides insight into the origins of TR errors. Using Parseval's theorem, the Fourier shift theorem, and the convolution theorem (Appendix A), denoting frequency by ν, and denoting the Fourier transform by a hat, we can transform the expression (7) for the variance of TR errors into the frequency domain as

$$\left\langle \theta^2 \right\rangle = \frac{1}{\tau_0} \int_0^{\infty} \left| \hat{\Pi}(\nu, \tau_x) - e^{-2\pi i \nu \Delta} \cdot \hat{\Pi}(\nu, \tau_a) \cdot \hat{\Pi}(\nu, \tau_y) \right|^2 |\hat{r}(\nu)|^2 d\nu. \tag{11}$$

The integrand of (11) is the product of two components. The second, $|\hat{r}(\nu)|^2$, is the power spectral density of $r(t)$, which describes the variance contained at frequencies in $r(t)$. The first component is a so-called power transfer function,

$$H(\nu) = \left| \hat{\Pi}(\nu, \tau_x) - e^{-2\pi i \nu \Delta} \cdot \hat{\Pi}(\nu, \tau_a) \cdot \hat{\Pi}(\nu, \tau_y) \right|^2, \tag{12}$$

which describes how power at different frequencies in $r(t)$ contributes to $\left\langle \theta^2 \right\rangle$. The Fourier transform of the boxcar function is a sinc function,

$$\hat{\Pi}(\nu, \tau) = \mathrm{sinc}(\tau\nu) = \frac{\sin(\pi\tau\nu)}{\pi\tau\nu}, \tag{13}$$

which converges towards 1 at frequencies below $1/\tau$ and oscillates with decreasing amplitude about 0 at higher frequencies (Figure 2a).

The function $H(\nu)$ describes which frequencies in a climate signal contribute most to TR errors. The largest values in $H(\nu)$ lie within a frequency band (Figure 2b) that can be described by low and high "cutoff frequencies" $\nu_{low}^{\dagger}$ and $\nu_{high}^{\dagger}$ at which

Clim. Past Discuss., https://doi.org/10.5194/cp-2019-10
Manuscript under review for journal Clim. Past
Discussion started: 11 February 2019

$H(\nu) = 1/2$. Cutoff frequencies can be approximated by assuming zero time offsets ($\Delta = 0$) and assuming that τ_x and τ_y are sufficiently separated ($\tau_x \geq 4\tau_y$ appears to be a rule of thumb) that

$$H\left(\nu^{\dagger}_{low}\right) \approx \left|\mathrm{sinc}^2\left(\tau_x \nu^{\dagger}_{low}\right) - 1\right|^2 = \tfrac{1}{2} \tag{14}$$

$$H\left(\nu^{\dagger}_{high}\right) \approx \left|\mathrm{sinc}\left(\tau_y \nu^{\dagger}_{high}\right)\right|^2 = \tfrac{1}{2}. \tag{15}$$

Solving these expressions yields $\nu^{\dagger}_{low} = 0.755\tau_x^{-1}$ and $\nu^{\dagger}_{high} = 0.443\tau_y^{-1}$. When τ_x is less than τ_y, these values are switched. If the paleoclimate archive was smoothed prior to sampling, then the expression for $\nu^{\dagger}_{high}$ becomes

$$H\left(\nu^{\dagger}_{high}\right) = \left|\mathrm{sinc}\left(\tau_a \nu^{\dagger}_{high}\right)\mathrm{sinc}\left(\tau_y \nu^{\dagger}_{high}\right)\right|^2 = \frac{1}{2}. \tag{16}$$

Solving using a Taylor series representation gives

$$\nu^{\dagger}_{high} \approx \frac{0.443}{\sqrt{\tau_a^2 + \tau_y^2}}, \tag{17}$$

which illustrates a combined effect from sampling and archive smoothing for determining which frequencies contribute to TR errors.

When there is a time offset, the band of nonzero values in $H(\nu)$ can extend to frequencies as low as $1/2\Delta$, with sinusoidal variations at time scales set by Δ (Figure 2d; Appendix A). In subsequent sections we will express chronological uncertainty in paleoclimate measurements by allowing Δ to be a random variable with probability distribution $p(\Delta)$. Given chronological uncertainty, we can compute a typical value for $\langle\theta^2\rangle$ by computing the expectation over $p(\Delta)$, denoted with a second pair of angle brackets,

$$\left\langle\left\langle\theta^2\right\rangle\right\rangle = \int_{-\infty}^{\infty} p(\Delta)\left\langle\theta^2\right\rangle d\Delta. \tag{18}$$

2.3 Practical implications from the simple model

Given estimates of the sampling interval, archive smoothing time scale, measurement offset, and an estimate of the signal spectrum, (11) is a closed-form expression for estimating TR errors in time-mean estimates. This equation provides a basis for some intuitive conclusions about errors and their implications for record sampling and uncertainty quantification:

1. TR errors can be traced to variability within a frequency band in $r(t)$ that is aliased onto time means. For instance, if a centennial mean is used to represent a millennial mean, in the absence of archive smoothing, the expected error variance is equal to the variance in $r(t)$ at periods between 226 and 1325 years (Figure 2). The error is the same if a centennial mean is used to represent a decadal mean.

2. The combined effects of archive smoothing and sampling can lead to over-smoothing. For instance, choosing a sampling interval τ_y equal to τ_x when $\tau_a > 0$ will over-smooth a record and lead to errors because the observed quantity averages over a longer interval than the target.

Clim. Past Discuss., https://doi.org/10.5194/cp-2019-10
Manuscript under review for journal Clim. Past
Discussion started: 11 February 2019

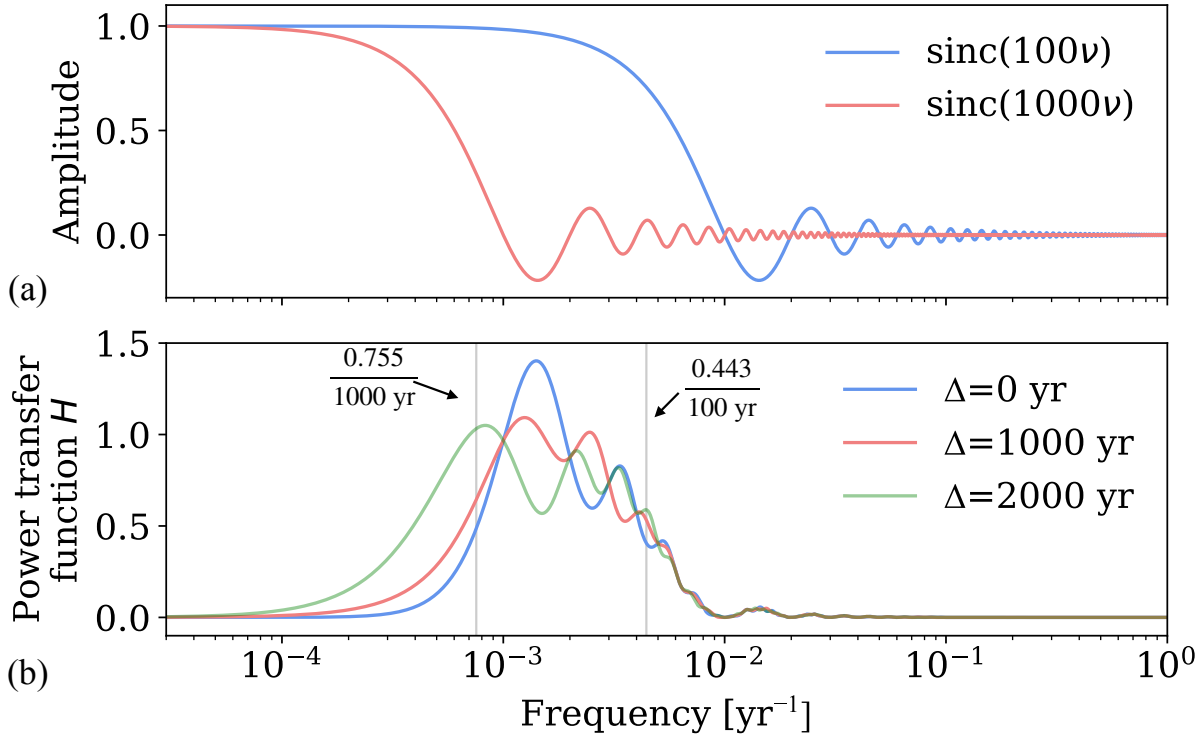

Figure 2. Contributions to the power transfer function H (Equation 12) illustrate the dependence of temporal representativeness errors on sampling time scales. (a) The Fourier transform of the boxcar function (Equation 2) is the sinc function (Equation 13), illustrated here for $\tau = 100$ and $\tau = 1000$. (b) Power transfer function computed with $\tau_x = 1000$, $\tau_y = 100$, and three different values of the time offset Δ. When $\Delta = 0$, Equations (14) and (15) approximate the edges of the frequency band in $r(t)$ that is aliased onto errors θ. For nonzero Δ, errors originate from frequencies as low as $1/(2\Delta)$.

Clim. Past Discuss., https://doi.org/10.5194/cp-2019-10
Manuscript under review for journal Clim. Past
Discussion started: 11 February 2019

3. We can estimate an ideal sampling interval $\tilde{\tau}_y$ in the presence of archive smoothing by minimizing the width of the frequency band that contributes to TR error. Setting $0.443\tilde{\tau}_x^{-1} = 0.443(\tau_y^2 + \tau_a^2)^{-\frac{1}{2}}$ and solving yields

$$\tilde{\tau}_y = \sqrt{\tau_x^2 - \tau_a^2} \text{ for } \tau_x > \tau_a. \tag{19}$$

Subsequent experiments (Figure 5) show that this approximation is robust across different parameters.

4. When there is a time offset in the measurement relative to the target, additional variability is aliased onto errors.

3 Application: Estimating errors at the Last Glacial Maximum

Next the error model is applied in the context of a particular mean estimation problem: the Last Glacial Maximum (LGM), the period roughly 20,000 years ago that is associated with the greatest land ice extent during the last glacial period. Following MARGO Project Members (2009) and others, LGM properties are defined to be estimates of time means over the 4000-year-long period from 23,000 to 19,000 years ago (23-19 kya). To estimate LGM errors, we will estimate the typical errors that would arise in the case of representing a 4000-year long interval centered on 21 kya.

Denote the time-mean value of a climate quantity $r(t)$ during the LGM as the target quantity x_{LGM},

$$x_{LGM} = \frac{1}{4000} \int_{-23{,}000}^{-19{,}000} r(t)\, dt.$$

To illustrate TR errors, we will compare averages over different time periods to x_{LGM}. For instance, consider a 1000-year time-mean value of $r(t)$ centered on 19.5 kya,

$$y_{LGM} = \frac{1}{1000} \int_{-19{,}000}^{-20{,}000} r(t)\, dt. \tag{20}$$

Such an estimate – dated to within the LGM, but averaging over only a subset – could reasonably be included in a binned-average compilation of LGM data. However, without accounting for errors resulting from the short averaging interval and time offset from the center of the LGM, we would expect this observation to bias a binned average. Similarly, were we to compare y_{LGM} to an LGM-mean estimate of $r(t)$ from a model without taking TR errors into account, we might erroneously conclude that the model did not fit the data.

To compare the effects of various time scales and spectra it is helpful to analyze a normalized version of $\langle \theta^2 \rangle$: the noise-to-signal standard deviation ratio,

$$f = \frac{\sqrt{\langle \theta^2 \rangle}}{\sigma_{\tau_c}}. \tag{21}$$

Because a common goal of LGM reconstructions is estimating glacial differences from modern climate, we adopt as our "signal" amplitude the expected anomaly σ_{τ_c} between two mean intervals of length τ_x separated by a time τ_c, where $\tau_c = 21{,}000$ years.

Clim. Past Discuss., https://doi.org/10.5194/cp-2019-10
Manuscript under review for journal Clim. Past
Discussion started: 11 February 2019

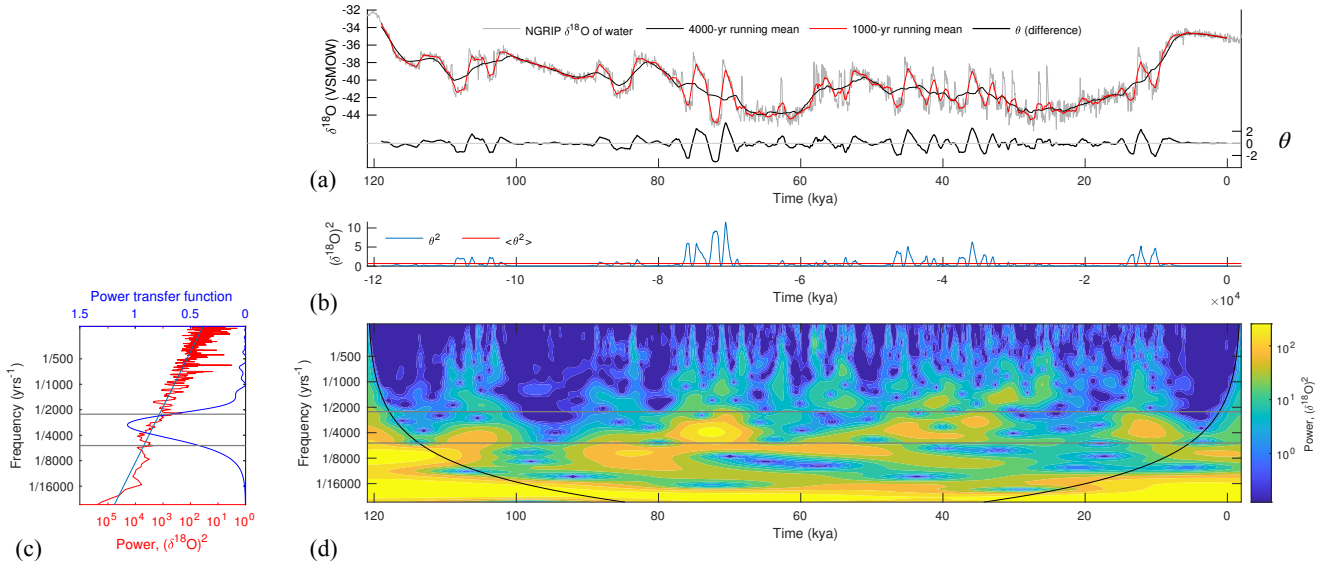

Figure 3. Temporal representativeness error in the time and frequency domains. Errors in representing a 4000-year mean by a 1000-year mean are estimated by computing the difference θ ((a), thick black line) between a 4000-year (red line) and 1000-year (thin black line) running mean of the NGRIP $\delta^{18}O_{ice}$ record (grey). The time average (red line, (b)) of θ^2 (blue line) is an estimate (0.7, units of $\left(‰\delta^{18}O\right)^2$) of the temporal representativeness error variance. Large values in θ^2 correspond to time periods with increased variability, as diagnosed by a wavelet analysis (d), particularly in the band between 2257 and 5298 year periods (grey lines). These periods correspond to $1/\nu^{\dagger}_{low}$ and $1/\nu^{\dagger}_{high}$, the reciprocals of the lower and upper cutoff frequencies for the power transfer function (dark blue curve, (c)). The light blue line in panel (c) indicates a power spectrum of the form $\nu^{-\beta}$ with $\beta = 1.53$ derived by a least-squares fit to the NGRIP spectrum.

3.1 Analysis of errors by subsampling a high-resolution paleoclimate record

To study the sensitivities of TR errors to sampling time scales, we first compare different moving averages of a high-resolution climate record, the North Greenland Ice Core Project (NGRIP; Andersen et al. (2004)) 50-year average time series of oxygen isotope ratios ($\delta^{18}O$) of ice. Smoothing this record with running means of length $\tau_x = 4000$ and $\tau_y = 1000$ yields time series of target and observation values x and y (black and red lines, Figure 3a). Their difference is the error θ (thick black line, Fig. 3a); the mean $\langle\theta^2\rangle$ (red line, Figure 3b) of θ^2 (blue line, Fig. 3b) is 0.7 $\left(‰\delta^{18}O\right)^2$ and is our estimate of the error variance (corresponding to a typical deviation of $\sqrt{\langle\theta^2\rangle} = 0.8‰$). Errors in some time periods (including the LGM) are relatively small, whereas other times (e.g. 80-70 kya) have larger errors and contribute more to $\langle\theta^2\rangle$. This time-variability in errors arises from nonstationarities in the NGRIP oxygen isotope record and highlights limitations of the stationarity assumption in our analysis. Because error amplitudes vary in time, there will be a tendency to overestimate errors during some epochs and underestimated

Clim. Past Discuss., https://doi.org/10.5194/cp-2019-10
Manuscript under review for journal Clim. Past
Discussion started: 11 February 2019

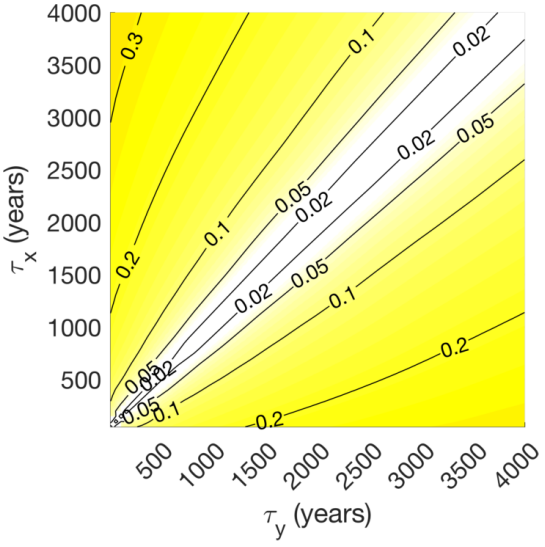

Figure 4. Error-to-signal variance fractions f (21) for estimates of time-mean values computed from the NGRIP record of Pleistocene oxygen isotopes contoured as a two-dimensional function of target averaging interval τ_x and observation averaging interval τ_y. A value of 0.1 means that TR error amplitudes are 10% of the "signal," defined as the typical difference between two intervals separated by 21,000 years.

them in others. Nevertheless, we maintain that the estimate of $\langle\theta^2\rangle$ is a reasonable characterization of typical error variance, particularly in the general case where information about nonstationarity is not be available.

Taking the square root of $\langle\theta^2\rangle$ and normalizing by σ_{τ_0}, which is estimated by taking the square root of the lag τ_c autocovariance estimated over the NGRIP record, gives us the noise-to-signal ratio f for ranges of τ_x and τ_y between 10 and 4000 years (Figure 4). Errors are zero for $\tau_x = \tau_y$ and increase monotonically away from those values. Absolute errors $\langle\theta^2\rangle$ are symmetric (i.e., equal if τ_x and τ_y are interchanged, not shown), but asymmetry in f arises because σ_{τ_0} depends on τ_x. TR errors can be up to 30% of signal amplitudes, with the largest errors occurring when a large τ_x is represented by a small τ_y. Thus, in the absence of archive smoothing, TR errors due to sampling procedures appear to contribute meaningfully to errors in estimates of past time-mean climate quantities.

3.2 Dependence on signal spectrum and archive smoothing

To investigate how TR errors depend on the spectral character of the climate processes being sampled, we shift our focus away from observations and assume power-law spectra for $r(t)$ having the form

$$|\hat{r}(\nu)|^2 \propto \nu^{-\beta}, \tag{22}$$

where $|\hat{r}(\nu)|^2$ is the power spectral density and β is the spectral slope (when plotted in log-log space, $\nu^{-\beta}$ is a straight line with slope $-\beta$). Spectra consistent with a power-law description are common in climate (Wunsch, 2003). Here we consider spectral slopes $\beta = 0.5$ and $\beta = 1.5$, motivated by Huybers and Curry (2006), who fit paleoclimate records to spectral slopes

Clim. Past Discuss., https://doi.org/10.5194/cp-2019-10
Manuscript under review for journal Clim. Past
Discussion started: 11 February 2019

Climate of the Past Discussions

between $\beta = 0.3$ and $\beta = 1.6$. Climatological spectral features that are not described by power laws, such as peaks due to the deterministic astronomical forcing from annual cycle or Milankovich variability, can also contribute to errors (Pisias and Mix, 1988; Wunsch, 2000) but are not considered specifically in these examples. All calculations are performed by numerical integration of Equation (11) by global adaptive quadrature.

Figure 5 shows the dependence of the noise-to-signal ratio f on the target interval length τ_x and the sampling interval length τ_y, varying the archive smoothing time scale τ_a to be 0 and 1000 years, and varying the spectral slope β to be 0.5 and 1.5. The close resemblance between Figure 5b (with $\beta = 1.5$) and the corresponding figure (4) computed in the time domain from NGRIP, which has spectral slope of 1.53 (Figure 3c), is partly coincidental; analysis of synthetic records with spectral slopes of 1.5 (not shown) reveals variability in f because of variations about the power law distribution in finite-length, stochastically generated time series. Nevertheless, the agreement shows correspondence between time-domain and spectral approaches.

In the cases with no archive smoothing ($\tau_a = 0$, Figures 5a and 5b), errors are minimized for $\tau_x = \tau_y$ and increase monotonically away from those values. Errors are greatest for small values of τ_y and large values of τ_x, where TR error can dwarf the relatively small signal amplitudes that are typical of 21,000-year differences in long-term time averages. As spectra become more "red" (here, $\beta = 1.5$ rather than $\beta = 0.5$), the signal amplitude σ_{τ_c} increases relative to $\langle \theta^2 \rangle$, and f decreases, as discussed also by Wunsch (1978) and Wunsch (2003). Introducing archive smoothing (Figures 5a and 5c, shown for the case of τ_a=1000), primarily affects f for $\tau_y < \tau_a$. In that regime, the largest values of f for small τ_y are reduced because archive smoothing serves as an anti-aliasing filter. Moreover, values of τ_y that minimize f change to reflect contributions from over-smoothing; for instance, when $\tau_x = 1000$, $\tilde{\tau}_y$ is close to zero. Observational averaging lengths τ_y that minimize f both with and without smoothing are well predicted by Equation (19) (dotted lines, Figure 5).

3.3 Effects from known and unknown chronological offsets

Offsets Δ between observed and target intervals aliases frequencies greater than $1/2\Delta$ onto the mean and modulates errors due to τ_x, τ_y, and τ_a (Section 2.2, Appendix A). Figure 6 illustrates these effects by computing f for $\tau_x = 4000$ years and varying Δ, τ_y, τ_a, and β. In all cases, errors grow monotonically away from the values $\Delta = 0$, $\tau_y = \tau_x$. For a given value of τ_y, the sensitivity of f to Δ (visible as a kink in contours, particularly in Figure 6a) increases for $\Delta > \left|\tau_x - \tau_y\right|/2$, when the observed time period begins to fall outside the target interval. As before, errors are more pronounced for $\beta = 0.5$ than for $\beta = 1.5$, with errors larger than the signal for small values of τ_y at all values of Δ for $\beta = 0.5$, reflecting the smaller amplitude of aliased variability relative to σ_{τ_c}. Archive smoothing reduces f for $\tau_y < \tau_a$; for $\tau_y > \tau_a$, archive smoothing has no qualitative effect in the parameter range shown.

When the dating of a measurement is uncertain, a range of Δ values may be possible, as specified by a probability distribution function $p(\Delta)$. To explore a scaling of the effects from chronological uncertainty on representational error, we assume that $p(\Delta)$ is Gaussian about zero with standard deviation equal to the time scale σ_Δ. We then compute f as $\sqrt{\langle\langle\theta^2\rangle\rangle}/\sigma_{\tau_0}$, where $\langle\langle\theta^2\rangle\rangle$ is given by numerical integration of Equation (18). In practice, $p(\Delta)$ can adopt a range of shapes, and in some cases (e.g., from radiocarbon ages; Telford et al. (2004)) can be non-Gaussian and/or bimodal, which would introduce additional time scales and could qualitatively change results. Such errors can be investigated by integrating Equation (18) with a non-Gaussian $p(\Delta)$.

Clim. Past Discuss., https://doi.org/10.5194/cp-2019-10
Manuscript under review for journal Clim. Past
Discussion started: 11 February 2019

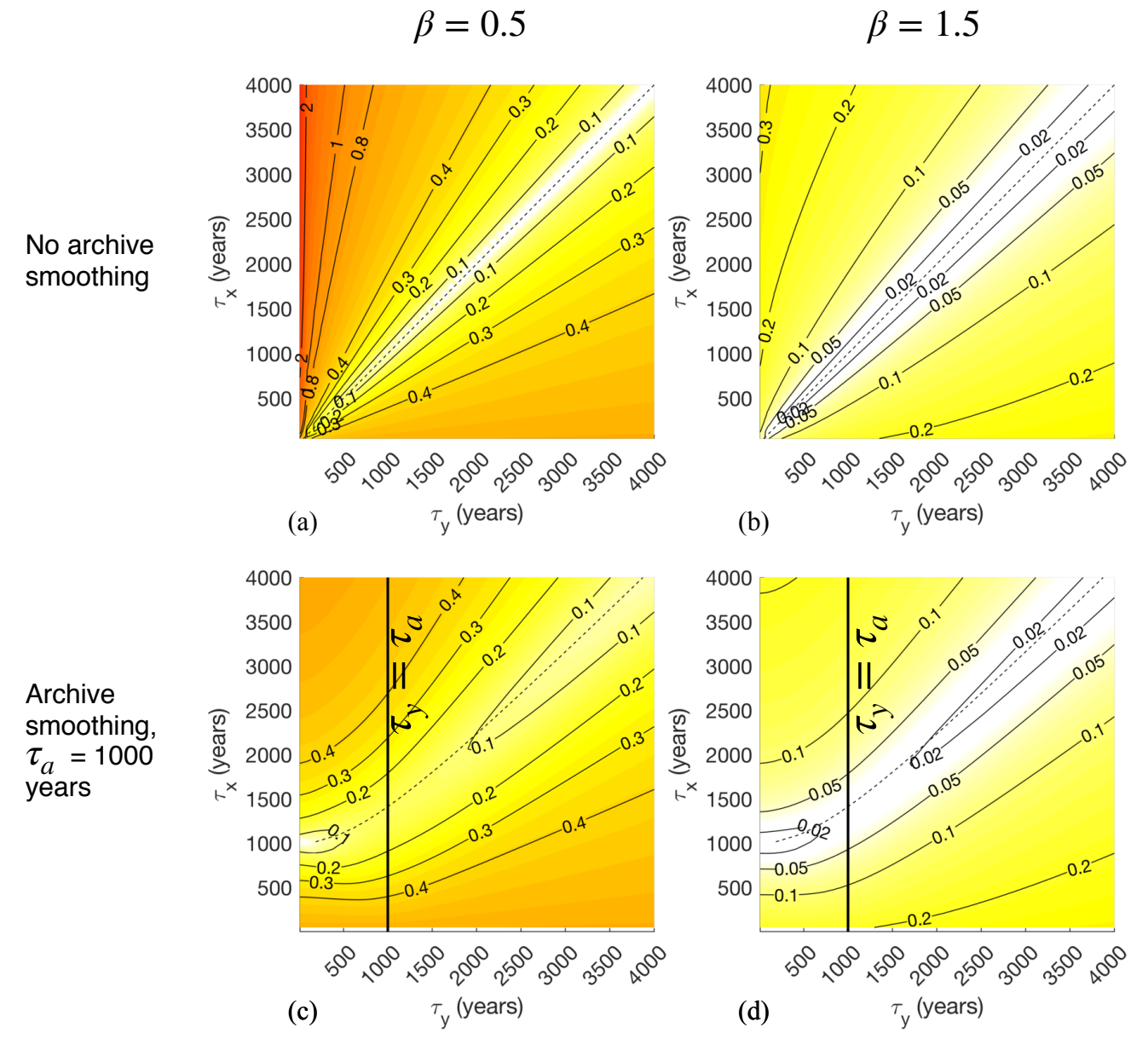

Figure 5. Error-to-signal fractions f for time-mean estimates plotted as a function of target averaging interval τ_x and observation averaging interval τ_y. Climate signal spectra are approximated as power law functions of frequency ($|\hat{r}(\nu)|^2 \propto \nu^{-\beta}$) with spectral slopes β equal to 0.5 (left column) and 1.5 (right column). The top row corresponds to a case with no archive smoothing ($\tau_a = 0$) while the bottom row corresponds to a case where the signal $r(t)$ is smoothed by a running mean over $\tau_a = 1000$ years. Time scales were chosen to be relevant to the problem of time-mean estimation at the Last Glacial Maximum, ca. 20 kya. Dotted lines show values of $\tilde{\tau}_y$ derived to minimize error estimated according to Equation (19).

Clim. Past Discuss., https://doi.org/10.5194/cp-2019-10
Manuscript under review for journal Clim. Past
Discussion started: 11 February 2019

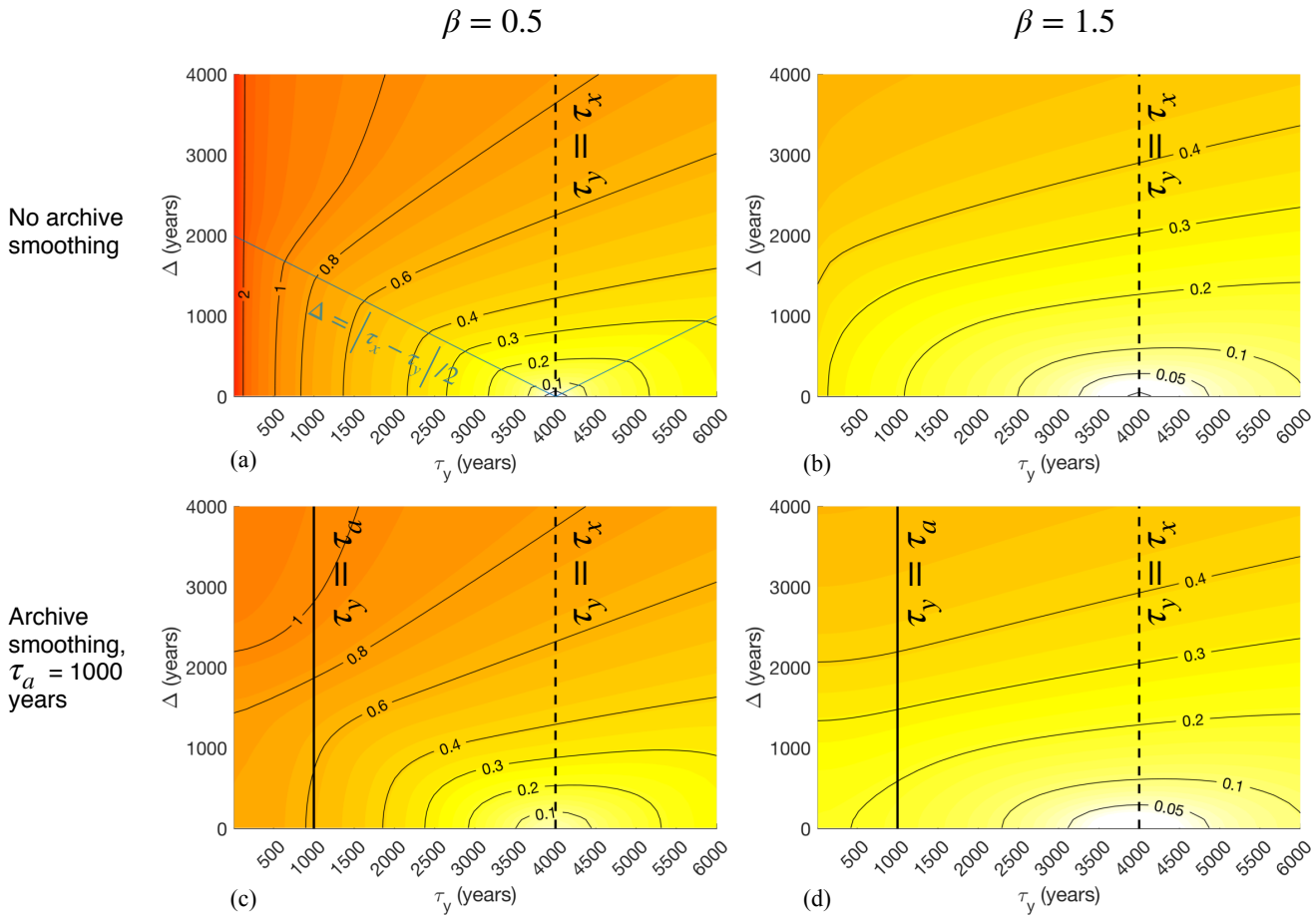

Figure 6. Same as Figure 5, but illustrating effects of offsets Δ between target and observational intervals on noise-to-signal ratios. Error fractions f are plotted as a function of the observational averaging interval τ_y and the standard deviation σ_Δ of a Gaussian distribution of observational offset centered on zero. In all cases, the target averaging interval is $\tau_x = 4000$, reflecting the nominal length of the Last Glacial Maximum. Values along the line $\tau_y = \tau_x$ strictly reflect the influence of chronological offsets. The blue line in panel (a) denotes values for which $\Delta = |\tau_x - \tau_y| /2$, indicating the maximum values of Δ for which τ_x and τ_y completely overlap.

Clim. Past Discuss., https://doi.org/10.5194/cp-2019-10
Manuscript under review for journal Clim. Past
Discussion started: 11 February 2019

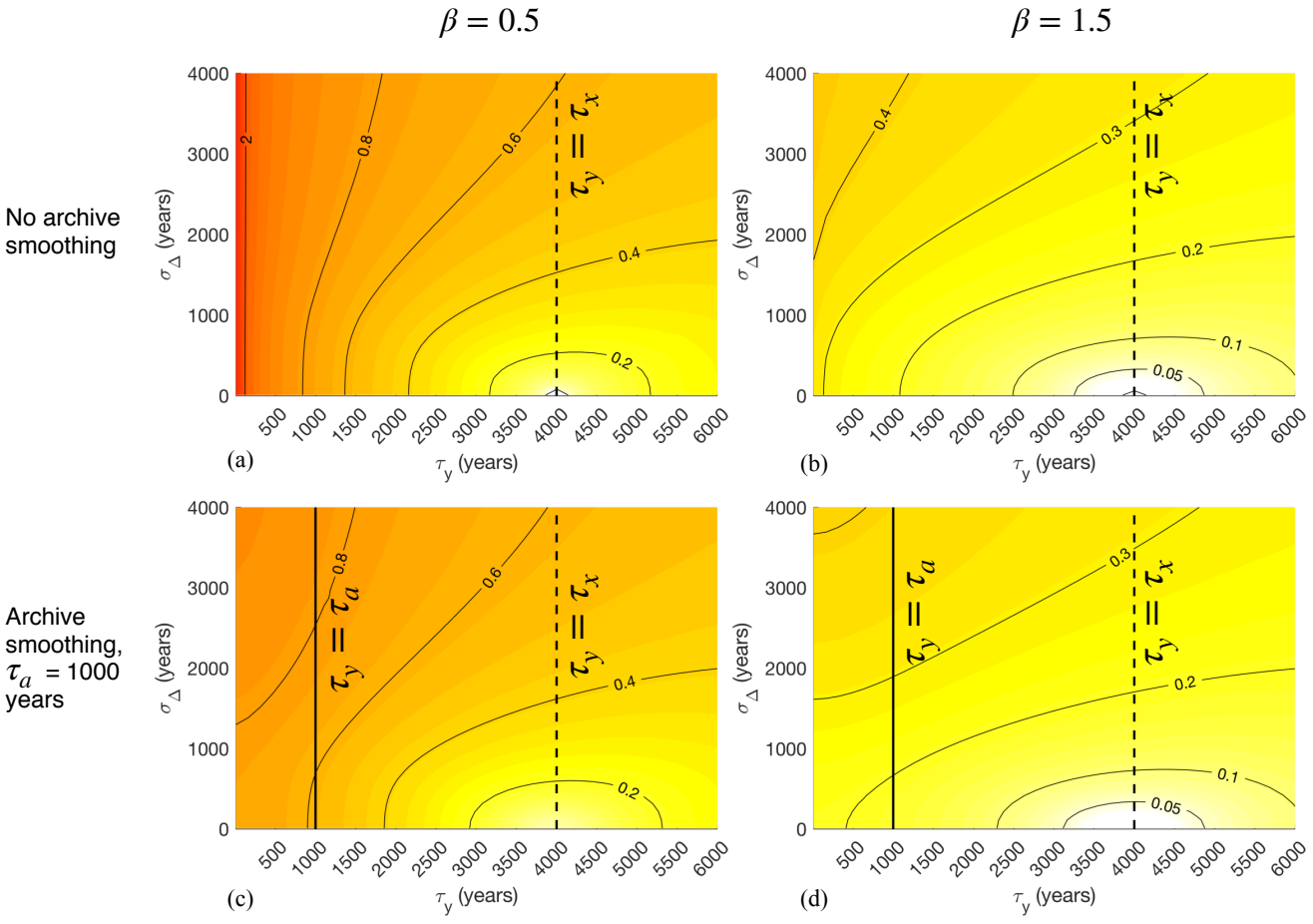

Figure 7. Same as Figure 5, but illustrating effects of chronological uncertainties in observations on noise-to-signal ratios. Error fractions f are plotted as a function of the observational averaging interval τ_y and the standard deviation σ_Δ of a Gaussian distribution of time offsets centered on zero. In all cases, the target averaging interval is $\tau_x = 4000$, reflecting the nominal length of the Last Glacial Maximum. Values along the line $\tau_y = \tau_x$ strictly reflect the influence of chronological uncertainty, which is zero when the observational offset is exactly known to be zero, (i.e., $\sigma_\Delta = 0$).

Expected errors f as a function of σ_Δ and τ_y (Figure 7) are qualitatively similar to those for Δ and τ_y (Figure 6), though values are everywhere slightly reduced, and the transition in sensitivity to σ_Δ across $\sigma_\Delta = |\tau_x - \tau_y|/2$ is less pronounced than for the equivalent in Figure 6, as is expected given that a range of lags is possible for any nonzero σ_Δ. A consequence is that TR error arising from a chronological offset that is unknown, with standard deviation N years, is similar to the error arising from a known chronological offset of N years. This similarity holds in the presence of archive smoothing.

Clim. Past Discuss., https://doi.org/10.5194/cp-2019-10
Manuscript under review for journal Clim. Past
Discussion started: 11 February 2019

Climate of the Past Discussions

4 Extension to time series analysis

Paleoclimate time series are sequences of time-mean values. Just as sampling, archive smoothing, and time offsets can introduce errors in estimates of time mean properties, so too do they introduce errors in time series. However, these errors differ from the time mean case because, as discussed below, uniform time mean measurements are not ideal for constructing time series. Here we adapt the TR machinery to analyze individual measurements in paleoclimate time series. We show that in the absence of archive smoothing, dense sampling (i.e., setting the averaging interval equal to the spacing between measurements) is a nearly optimal approach to minimize TR errors.

The sampling theorem of Shannon (1949) states that sampling $r(t)$ instantaneously (that is, with a very short averaging interval) at times separated by a fixed time interval τ_s unambiguously preserves signal information only when $r(t)$ does not contain any spectral power at frequencies greater than $1/2\tau_s$ (called the Nyquist frequency, ν_{Nyq}). When this criterion is not met, the discrete signal is corrupted by aliasing, whereby variability in $r(t)$ at frequencies greater than ν_{Nyq} appears artificially at lower frequencies in the discrete signal. To mitigate aliasing, one can either increase the sampling rate or apply a low-pass "anti-aliasing" filter to $r(t)$ to attenuate power at frequencies higher than ν_{Nyq}. In the process of constructing a paleoclimate time series, sampling time-mean values yields a moving average that serves as an anti-aliasing filter. Thus we expect sample averaging procedures to affect aliasing errors in time series, as also discussed by von Albedyll et al. (2017).

We will use Shannon's theorem to obtain a frequency-domain expression for TR errors for individual time series measurements. Our procedure is to 1) define local (in time) values of τ_s^i and ν_{Nyq}^i for the i^{th} observation and 2) compute the expected errors if an entire time series were sampled using those local properties. To do this, we make the assumption that the sampling interval τ_s^i is locally constant: that is, for the i^{th} measurement y^i taken at time t^i, y^{i-1} was taken at time $t^i - \tau_s^i$, and y^{i+1} was taken at time $t^i + \tau_s^i$. If the sampling interval changes rapidly, conclusions from this approach might not apply.

Define the moving average time series associated with y^i to be

$$y^i(t) = \Pi\left(t, \tau_y^i\right) \star \Pi\left(t, \tau_a^i\right) \star r(t) \tag{23}$$

where we have included a contribution from archive smoothing, so that its Fourier transform is

$$\hat{y}^i(\nu) = \hat{\Pi}\left(\nu, \tau_y^i\right) \cdot \hat{\Pi}\left(\nu, \tau_a^i\right) \cdot \hat{r}(\nu). \tag{24}$$

By Shannon's theorem, an accurate discrete representation of $r(t)$ results from sampling all frequencies in $r(t)$ less than or equal to the local Nyquist frequency $\nu_{Nyq}^i = 1/\left(2\tau_s^i\right)$. As such, the target value x^i for the i^{th} measurement y^i is the value of $r(t)$ sampled at t^i after filtering $r(t)$ to remove high-frequency variability. The Fourier transform of a time series of values of x^i is

$$\hat{x}^i(\nu) = G\left(\nu, \tau_s^i\right) \hat{r}(\nu) \tag{25}$$

where the "ideal" transfer function $G(\nu, \tau_s)$ is the piecewise constant Heaviside function

$$G(\nu, \tau_s) = \begin{cases} 1 & \nu < 1/(2\tau_s^i) \\ 0 & \nu \geq 1/\left(2\tau_s^i\right) \end{cases} \tag{26}$$

Clim. Past Discuss., https://doi.org/10.5194/cp-2019-10
Manuscript under review for journal Clim. Past
Discussion started: 11 February 2019

Climate of the Past Discussions

that is ideal in the sense that it eliminates variability at frequencies greater than $\nu_{Nyq}^{i} = 1/\left(2\tau_s^i\right)$. Then we define TR error at the i^{th} measurement to be

$$\theta^i = x^i - y^i. \tag{27}$$

As in the previous section, we estimate the variance of θ^i by taking the expected value as if the entire record had been sampled using the local values τ_s^i and τ_y^i. Then, equivalent to (11),

$$\left\langle \theta^{i2} \right\rangle = \frac{1}{\tau_0} \int_0^\infty \left| G\left(\nu, \tau_s^i\right) - \hat{\Pi}\left(\nu, \tau_a^i\right) \cdot \hat{\Pi}\left(\nu, \tau_y^i\right) \right|^2 |\hat{r}(\nu)|^2 \, d\nu. \tag{28}$$

Similar to the time-mean case, $\left\langle \theta^{i2} \right\rangle$ is a weighted integral over the power density spectrum of $r(t)$. Weights are largest at frequencies between ν_{Nyq} and either $\nu_{low}^{\dagger}$ (if $\tau_y > \tau_s$) or $\nu_{high}^{\dagger}$ (if $\tau_y < \tau_s$). Unlike in the mean estimation case, where TR errors can be zero, nonzero error is unavoidable with uniform sampling because of differences between the shape of the sinc function and the abrupt frequency cutoff specified by $G\left(\nu, \tau_s^i\right)$. Sampling a paleoclimate archive nonuniformly in time could better approximate the ideal filter and reduce errors, but this may not be practical given the many other sources of error in paleoclimate records.

To demonstrate sensitivities to parameters we again compute noise-to-signal ratios. We take signal strength to be the estimated standard deviation $\tilde{\sigma}_{x^i}$ of the time series of x^i (the ideally-sampled signal, defined in (25)), so that the noise-to-signal ratio at the i^{th} measurement is

$$f^i = \frac{\sqrt{\left\langle \theta^{i2} \right\rangle}}{\tilde{\sigma}_{x^i}}.$$

Because $\tilde{\sigma}_{x^i}$ can grow as a function of time series length for power-law spectra, we choose 21,000 years as the period over which to integrate signal variance, the approximate duration of the last deglaciation.

While the dependence of f^i on τ_s^i and τ_y^i (Figure 8) is qualitatively similar to the dependence on τ_x and τ_y in the time mean estimation case (Figure 5), there are some differences. First, as discussed above, errors are always 10% or more of signal amplitudes because of errors arising from constructing a time series as a sequence of time mean values. Second, values of τ_y that minimize errors do not obey $\tau_y = \tau_s$, but are larger by a factor of roughly 1.2, suggesting that samples should ideally span an interval slightly longer than the sampling interval. In practice, sampling densely (without space between observations) seems to be a good approximation of this error minimizing strategy. For time series constructed from short time averages spaced out by larger intervals in time, errors can be large relative to climate signals.

As stated above, these results hold for time series whose spacing and chronologies are not changing too rapidly and where the goal is to obtain a discrete representation of a continuous process. For other objectives, other sampling procedures may be preferred. For instance, "burst sampling," whereby rapid sequences of observations are taken at relatively long intervals, is used in modern oceanographic procedures to estimate spectral nonstationarities in time (Emery and Thomson, 2014), and unevenly spaced paleoclimate observations can be leveraged to give a range of frequency information using variogram approaches (Amrhein et al., 2015) or the Lomb-Scargle periodogram (e.g., Schulz and Stattegger, 1997). The danger of aliasing

Clim. Past Discuss., https://doi.org/10.5194/cp-2019-10
Manuscript under review for journal Clim. Past
Discussion started: 11 February 2019

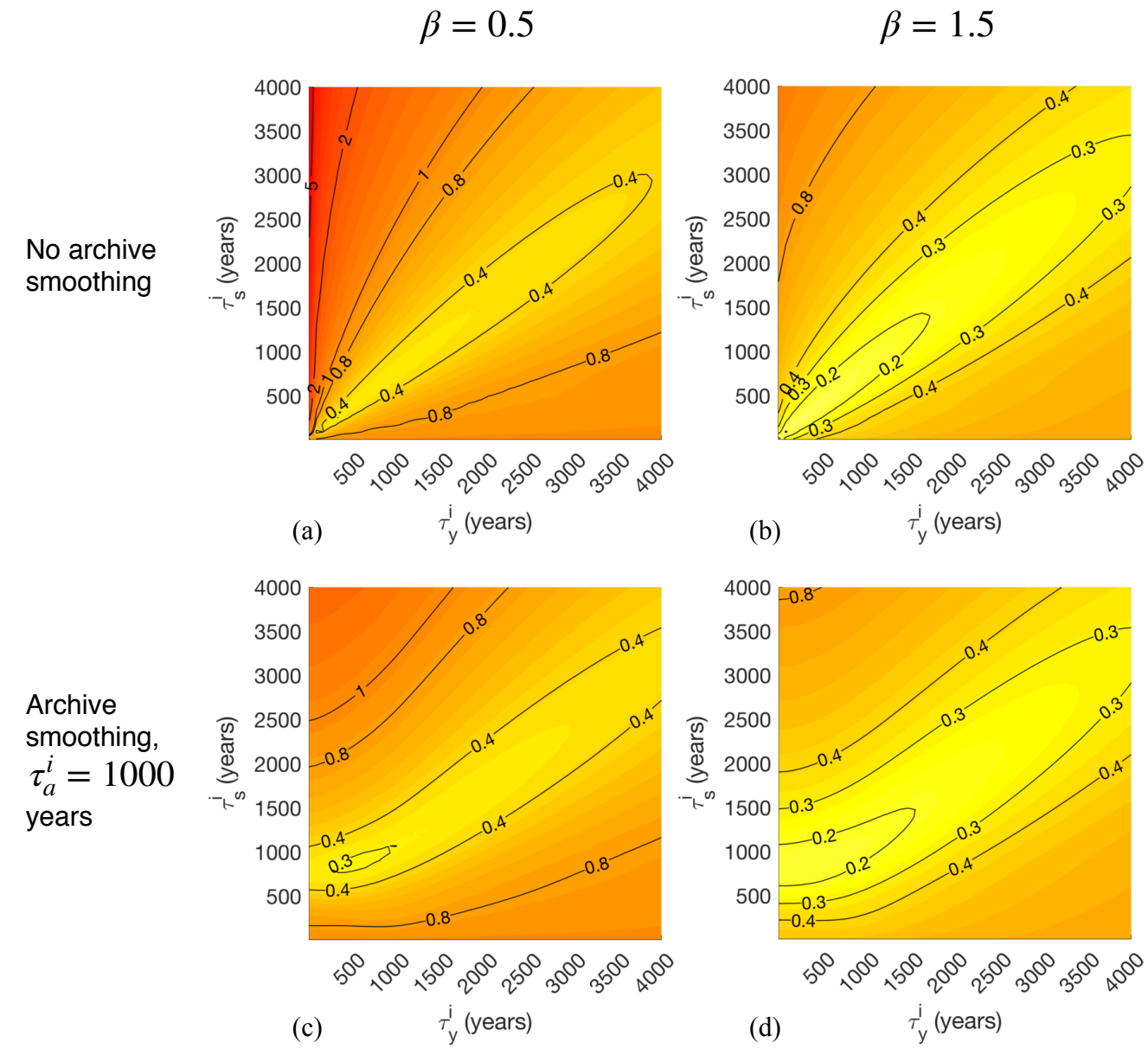

Figure 8. Same as Figure 5, but illustrating the dependence of the error-to-signal standard deviation ratio for individual measurements in a time series as a function of local time series spacing (τ_s^i) and the observational averaging time interval τ_y^i.

Clim. Past Discuss., https://doi.org/10.5194/cp-2019-10
Manuscript under review for journal Clim. Past
Discussion started: 11 February 2019

is omnipresent, and necessitates careful consideration of the frequencies sampled by an observation and the frequencies the observation is being used to constrain.

5 Discussion

This paper presents a framework for quantifying temporal representativeness (TR) errors in paleoclimate, broadly defined as resulting when one time average is represented by another. A simple model illustrates interacting effects from record sampling procedures, chronological errors, and the spectral properties of the climate process being sampled.

Uncertainty quantification is important for interpreting records, comparing them to other data, and incorporating them into reconstructions using inverse modeling or data assimilation approaches. For instance, uncertainties play a crucial role in determining how observations to influence least-squares reconstructions of past climate: highly uncertain observations carry little weight, while those with low uncertainty have more power in dictating reconstruction features. In data intercomparisons, differing sampling strategies could contribute to disagreement among paleoclimate records obtained from different archives, while sampling errors could be correlated measurements obtained from a single set of samples; the combination of these effects could lead to artificially better agreement of properties within than between archives.

We find that for some cases of sampling time scales, archive smoothing, and climate spectra, TR errors are non-negligible, with noise-to-signal ratios greater than 1 in some cases where the observational interval τ_y is smaller than the target interval τ_x. TR errors result from aliasing climate variability onto time mean observations and can be mitigated to some degree by sampling procedures and by archive smoothing, both of which act as anti-aliasing filters. However, archive smoothing can also destroy information about climate variability, and the combined effects of sampling and smoothing can over-smooth a record and lead to increased errors. The effects from mismatches between τ_x and τ_y have similar amplitudes to uncertainties from chronological errors in the parameter space considered. Moreover, chronological and sampling errors interact, for instance in the way that errors grow more quickly as a function of chronological uncertainty amplitude when that uncertainty is likely to place a measurement outside of a target interval (Figure 7). Given that these error variances were estimated using parameters representative of the LGM, it seems possible that TR errors may explain some of the disagreement among proxy measurements within that time period (e.g., MARGO Project Members, 2009; Caley et al., 2014), though nonstationarities may cause TR errors to be overestimated for climate intervals like the LGM that appear to be quiescent relative to other time periods. Importantly, we do not claim that TR errors are the largest source of error for any particular proxy type or reconstruction problem, though they may be in some cases. The tools presented can be used to assess likely error amplitudes.

Though not the principal goal, these analyses provide a basis for sampling practices that minimize errors, for instance for avoiding oversmoothing through the combined effects of sampling and archive smoothing (Section 2.2 and Equation 19). When constructing paleoclimate time series, it is important to bear in mind not just the Nyquist frequency but the role of sampling time scales as an anti-aliasing filter; these considerations point to dense sampling (i.e., without space between contiguous samples) in order to minimize error in the absence of effects from archive smoothing (Section 4). However, many practical considerations motivate paleoclimate sampling strategies, and may outweigh the concerns described here. For instance, records sampled

Clim. Past Discuss., https://doi.org/10.5194/cp-2019-10
Manuscript under review for journal Clim. Past
Discussion started: 11 February 2019

densely cannot be used as a starting point for subsequently constructing higher-resolution records. Moreover, preservation of natural archives for subsequent analyses is important for reproducibility and for sharing resources between laboratories, and may be complicated by continuous sampling.

To some extent, the simple model for TR error can be generalized to more complex scenarios. If samples are nonuniform in time – for instance, due to large changes in chronology, or because material was sampled using a syringe or drill bit with a circular projection onto an archive – then the sinc function in (11) can be replaced by Fourier transforms of the relevant functions. Similarly, a more complex pattern of archive smoothing can be accommodated by substituting a different smoothing kernel. Non-Gaussian age uncertainties can be incorporated by substituting a different distribution in (18). Changes in sampling properties through time (as might arise from non-constant chronologies or sampling procedures) can readily be accommodated because all computations are performed on a point-by-point basis. If sampling or smoothing time scales are unknown, a similar procedure can be adopted as was used for Δ in (18), whereby a second integration is performed to compute the expectation over an estimated probability distribution of one or more time scales.

Several caveats apply to the uncertainty estimates. First, the model neglects some processes that may be important. For instance, we assume that proxy archives store information continuously, thereby neglecting errors due to small numbers of foraminifera in sediment cores or particle size sorting in diagenesis. Second, nonstationarity in record spectra leads to time variations in errors, as illustrated in Figure 3. Third, by estimating errors for individual measurements, we ignore error covariances in time, which can result from chronologies constructed by interpolating ages between tie points; more complete characterizations could be achieved by Monte Carlo sampling of age model uncertainty (Anchukaitis and Tierney, 2013). More broadly, there is clear need for comprehensive approaches in uncertainty quantification that can reveal interactions among the various sources of uncertainty in paleoclimate records. Forward proxy system models (e.g., Evans et al., 2013; Dee et al., 2015; Dolman and Laepple, 2018) are a promising way forward to assess uncertainties holistically.

Aliasing is not limited to the time domain, and similar procedures may be useful for quantifying errors due to spatial representativeness by considering how well proxy records can constrain the regional and larger scales typically of interest in paleoclimatology. An analogous problem is addressed in the modern ocean by Forget and Wunsch (2007), and Zhao et al. (2018) considered spatial representativeness in choosing how to weight deglacial radiocarbon time series in spatial bin averages. A challenge of any such approach is that the spatial averaging functions (analogous to our τ_y, but occupying three spatial dimensions) represented by proxy records are often not well known; Van Sebille et al. (2015), for instance, explores how ocean advection determines three-dimensional patterns represented by sediment core observations. Because spatial patterns and time scales of ocean and climate variability are linked, it may ultimately be necessary to consider the full, four-dimensional spatiotemporal aliasing problem.

The hope is that these procedures may prove useful for first-order practical uncertainty quantification, and scripts and functions used in making figures are provided (see link in the Acknowledgements). A challenge is estimating the signal spectrum $|\hat{r}|^2$, which itself can be affected by aliasing (Kirchner, 2005). One approach is to use spectra from other records that are more highly-resolved or were sampled densely, e.g. from a sediment core at an adjacent site, or a record believed to record similar climate variability. Alternately, measurements of archive properties that can be made cheaply and at high resolution – such as

Clim. Past Discuss., https://doi.org/10.5194/cp-2019-10
Manuscript under review for journal Clim. Past
Discussion started: 11 February 2019

Climate of the Past Discussions

magnetic susceptibility, wet bulk density, and other proxy properties that are routinely made on sediment cores – could prove useful for estimating $|\hat{r}|^2$ if those properties are related linearly to $r(t)$ (Herbert and Mayer, 1991; Wunsch and Gunn, 2003). Another challenge is that time scales that we have shown affect errors are often not published alongside paleoclimate datasets, thus turning systematic errors (where parameters like τ_y are known) into stochastic errors because a range of possible values must be explored. Publishing all available information about sampling practices, age model construction, and assessments of archive smoothing will greatly aid uncertainty quantification efforts.

Appendix A: Expressing temporal representativeness errors in the frequency domain

The Fourier transform will be written using the operator $\mathscr{F}$ and by a hat, and denoting frequency by ν,

$$\mathscr{F}(x(t)) \equiv \hat{x}(\nu) = \int_{-\infty}^{\infty} x(t)\, e^{-2\pi i \nu t} dt.$$

Parseval's theorem states that the integral of a squared quantity in the time domain is equal to the integral of the squared amplitude of the Fourier transform of that quantity, so that we can write (7) as

$$\left\langle \theta^2 \right\rangle = \frac{1}{\tau_0} \int_{-\infty}^{\infty} \left(m(t,\tau_x) - m(t+\Delta t, \tau_y) \right)^2 dt \tag{A1}$$

$$= \frac{1}{\tau_0} \int_{0}^{\infty} \left| \mathscr{F}\left[m(t,\tau_x) - m(t+\Delta t, \tau_y) \right] \right|^2 d\nu. \tag{A2}$$

By the Fourier shift theorem,

$$\mathscr{F}\left[m(t+\Delta, \tau_y) \right] = e^{-2\pi i \nu \Delta} \mathscr{F}\left[m(t, \tau_y) \right]. \tag{A3}$$

Then, by the linearity of the Fourier transform,

$$\left\langle \theta^2 \right\rangle = \frac{1}{\tau_0} \int_{0}^{\infty} \left| \hat{m}(\nu, \tau_y) - e^{-2\pi i \nu \Delta} \hat{m}(\nu, \tau_x) \right|^2 d\nu. \tag{A4}$$

By the convolution theorem, convolution in the time domain is equivalent to multiplication in the frequency domain, and vice versa. Thus, the Fourier transform of a time mean as defined in (3) is

$$\hat{m}(\nu, \tau) = \mathscr{F}\left[\Pi(t,\tau) \star r(t) \right] \tag{A5}$$

$$= \hat{\Pi}(\nu, \tau) \cdot \hat{r}(\nu). \tag{A6}$$

Substituting into (A4) yields

$$\left\langle \theta^2 \right\rangle = \frac{1}{\tau_0} \int_{0}^{\infty} \left| \hat{\Pi}(\nu, \tau_x) - e^{-2\pi i \nu \Delta} \cdot \hat{\Pi}(\nu, \tau_y) \right|^2 |\hat{r}(\nu)|^2 d\nu. \tag{A7}$$

We can represent smoothing prior to sampling by substituting a new climate signal, $r(t)$, with a running mean applied,

$$r'(t) = \Pi(t, \tau_a) \star r(t).$$

Clim. Past Discuss., https://doi.org/10.5194/cp-2019-10
Manuscript under review for journal Clim. Past
Discussion started: 11 February 2019

Climate of the Past Discussions

Substituting $\hat{r}'(\nu)$ into (A7) and applying the convolution theorem gives

$$\left\langle \theta^2 \right\rangle = \frac{1}{\tau_0} \int_0^\infty \left| \hat{\Pi}(\nu, \tau_x) - e^{-2\pi i \nu \Delta} \cdot \hat{\Pi}(\nu, \tau_a) \cdot \hat{\Pi}(\nu, \tau_y) \right|^2 |\hat{r}(\nu)|^2 \, d\nu. \tag{A8}$$

To isolate errors from a time offset Δ, consider the limit where τ_x, τ_y, and τ_a approach zero, corresponding to instantaneous observations in time, so that $\left\langle \theta^2 \right\rangle$ approaches

$$\left\langle \theta^2 \right\rangle = \frac{1}{\tau_0} \int_0^\infty \left| 1 - e^{-2\pi i \nu \Delta} \right|^2 |\hat{r}(\nu)|^2 \, d\nu. \tag{A9}$$

Expanding $\left|1 - e^{-2\pi i \nu \Delta}\right|^2$ and simplifying gives

$$\left\langle \theta^2 \right\rangle = \frac{1}{\tau_0} \int_0^\infty (2 - 2\cos(2\pi\nu\Delta)) |\hat{r}(\nu)|^2 \, d\nu \tag{A10}$$

so that the power transfer function is $H = 2 - 2\cos(2\pi\nu\Delta)$ and the expected error due to Δ is a cosinusoidally-weighted function of the signal power spectrum. H takes a minimum value of 0 at frequencies

$$\nu_{min} = 0, \frac{1}{\Delta}, \frac{2}{\Delta}, \ldots \frac{n}{\Delta}$$

for integer values of n; at these frequencies, measurements spaced by Δ in time are in phase and are therefore exactly correlated (Figure A1a). The weights take a maximum value of 4 at frequencies

$$\nu_{max} = \frac{1}{2\Delta}, \frac{3}{2\Delta}, \frac{5}{2\Delta}, \ldots \frac{n}{\Delta} + \frac{1}{2\Delta}$$

where measurements separated by Δ are always exactly out of phase (Figure A1b). At those frequencies, the underlying signal $r(t)$ is projected twofold onto the error, so that its variance contribution is multiplied fourfold. These variations in frequency contributions to error modulate effects from smoothing and sampling timescales, as illustrated in Figure 2b.

Acknowledgements. Thanks to LuAnne Thompson, Greg Hakim, Lloyd Keigwin, Cristi Proistecescu, Carl Wunsch, and Thomas Laepple for useful conversations. Comments from two anonymous reviewers in a previous round of reviews helped improve the manuscript. Support came from NOAA grant NA14OAR4310176 and an NSF postdoctoral fellowship. Wavelet software was provided by C. Torrence and G. Compo, and is available at URL: http://paos.colorado.edu/research/wavelets/. MATLAB code is available at https://github.com/amrhein/TR-code.

Clim. Past Discuss., https://doi.org/10.5194/cp-2019-10
Manuscript under review for journal Clim. Past
Discussion started: 11 February 2019

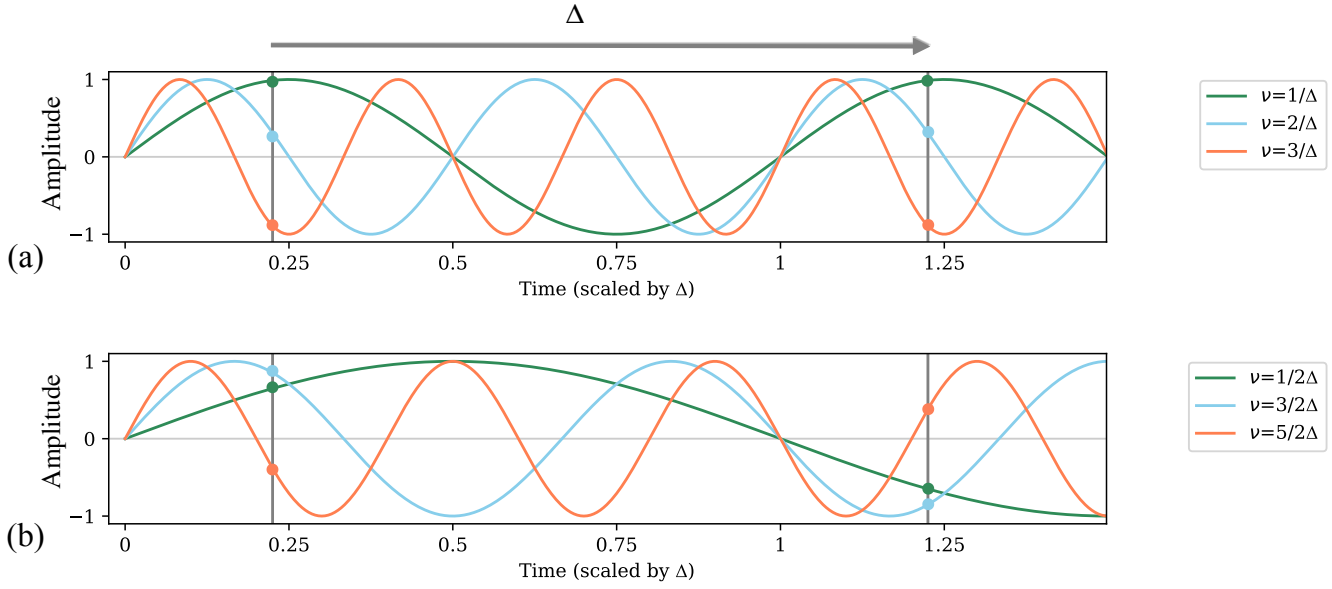

Figure A1. Illustration of the frequency dependence of errors in representing an instantaneous measurement of a process $r(t)$ at a time t by another measurement $r(t+\Delta)$. Each line represents a different frequency component of $r(t)$, grey vertical lines represent sampling times, and colored circles represent values of components at those times. At frequencies $\nu = \frac{n}{\Delta}$ for $n = 0, 1, 2, \ldots$, (a), the Fourier components of $x(t)$ will be exactly in phase when sampled at a time lag Δ, so these components do not contribute to the error variance $\left\langle (r(t) - r(t+\Delta))^2 \right\rangle$. By contrast, at frequencies $\nu = \frac{n}{\Delta} + \frac{1}{2\Delta}$ (b), the Fourier components are exactly out of phase, so these components tend to contribute most to the error variance. At intermediate frequencies, contributions lie between the two extremes, leading to a cosine function of error contribution as a function of frequency (Equation A10).

References

Adkins, J. F., Boyle, E. A., Curry, W. B., and Lutringer, A.: Stable isotopes in deep-sea corals and a new mechanism for "vital effects", Geochimica et Cosmochimica Acta, 67, 1129–1143, https://doi.org/10.1016/S0016-7037(00)01203-6, 2003.

Amrhein, D. E., Gebbie, G., Marchal, O., and Wunsch, C.: Inferring surface water equilibrium calcite δ 18 O during the last deglacial period from benthic foraminiferal records: Implications for ocean circulation, Paleoceanography, 30, 1470–1489, 2015.

Amrhein, D. E., Wunsch, C., Marchal, O., and Forget, G.: A Global Glacial Ocean State Estimate Constrained by Upper-Ocean Temperature Proxies, Journal of Climate, 31, 8059–8079, 2018.

Anchukaitis, K. J. and Tierney, J. E.: Identifying coherent spatiotemporal modes in time-uncertain proxy paleoclimate records, Climate Dynamics, 41, 1291–1306, https://doi.org/10.1007/s00382-012-1483-0, 2013.

Andersen, K. K., Azuma, N., Barnola, J.-M. M., Bigler, M., Biscaye, P., Caillon, N., Chappellaz, J., Clausen, H. B., Dahl-Jensen, D., Fischer, H., and Others: {H}igh-resolution record of {N}orthern {H}emisphere climate extending into the last interglacial period, Nature, 431, 147, 2004.

Anderson, D. M.: {A}ttenuation of millennial-scale events by bioturbation in marine sediments, Paleoceanography, 16, 352–357, 2001.

Beer, J., McCracken, K., and Von Steiger, R.: {C}osmogenic radionuclides: theory and applications in the terrestrial and space environments, Springer Science & Business Media, 2012.

Bronk Ramsey, C.: Bayesian Analysis of Radiocarbon Dates, Radiocarbon, 51, 337–360, https://doi.org/10.1017/S0033822200033865, https://www.cambridge.org/core/product/identifier/S0033822200033865/type/journal{_}article, 2009.

Buck, C. E.: Bayesian Chronological Data Interpretation: Where Now?, LECTURE NOTES IN STATISTICS-NEW YORK-SPRINGER VERLAG-, pp. 1–24, 2004.

Buck, C. E. and Millard, A.: Tools for constructing chronologies: crossing disciplinary boundaries, Springer Verlag, 2004.

Caley, T., Roche, D. M., Waelbroeck, C., and Michel, E.: {O}xygen stable isotopes during the {L}ast {G}lacial {M}aximum climate: perspectives from data–model (i{LOVECLIM}) comparison, Climate of the Past, 10, 1939–1955, 2014.

Clark, P. U., Shakun, J. D., Baker, P. A., Bartlein, P. J., Brewer, S., Brook, E., Carlson, A. E., Cheng, H., Kaufman, D. S., Liu, Z., and Others: {G}lobal climate evolution during the last deglaciation, Proceedings of the National Academy of Sciences, 109, E1134—-E1142, 2012.

Dee, S., Emile-Geay, J., Evans, M. N., Allam, A., Steig, E. J., and Thompson, D.: PRYSM: An open-source framework for PRoxY System Modeling, with applications to oxygen-isotope systems, Journal of Advances in Modeling Earth Systems, 7, 1220–1247, https://doi.org/10.1002/2015MS000447, http://doi.wiley.com/10.1002/2015MS000447, 2015.

Dolman, A. M. and Laepple, T.: Sedproxy: a forward model for sediment archived climate proxies, Climate of the Past Discussions, pp. 1–31, https://doi.org/10.5194/cp-2018-13, https://www.clim-past-discuss.net/cp-2018-13/, 2018.

Elderfield, H., Vautravers, M., and Cooper, M.: The relationship between shell size and Mg/Ca, Sr/Ca, δ ¹⁸ O, and δ ¹³ C of species of planktonic foraminifera, Geochemistry, Geophysics, Geosystems, 3, 1–13, https://doi.org/10.1029/2001GC000194, http://doi.wiley.com/10.1029/2001GC000194, 2002.

Emery, W. J. and Thomson, R. E.: {D}ata analysis methods in physical oceanography, Newnes, 2014.

Evans, M. N., Tolwinski-Ward, S. E., Thompson, D. M., and Anchukaitis, K. J.: {A}pplications of proxy system modeling in high resolution paleoclimatology, Quaternary Science Reviews, 76, 16–28, 2013.

Fairchild, I. J., Smith, C. L., Baker, A., Fuller, L., Spötl, C., Mattey, D., and McDermott, F.: Modification and preservation of environmental signals in speleothems, Earth-Science Reviews, 75, 105–153, https://doi.org/10.1016/j.earscirev.2005.08.003, 2006.

Forget, G. and Wunsch, C.: {E}stimated global hydrographic variability, Journal of Physical Oceanography, 37, 1997–2008, 2007.

Haam, E. and Huybers, P.: {A} test for the presence of covariance between time-uncertain series of data with application to the {D}ongge {C}ave speleothem and atmospheric radiocarbon records, Paleoceanography, 25, 2010.

Hakim, G. J., Emile-Geay, J., Steig, E. J., Noone, D., Anderson, D. M., Tardif, R., Steiger, N., and Perkins, W. A.: The last millennium climate reanalysis project: Framework and first results, Journal of Geophysical Research, 121, 6745–6764, https://doi.org/10.1002/2016JD024751, 2016.

Herbert, T. D. and Mayer, L. A.: {L}ong climatic time series from sediment physical property measurements, Journal of Sedimentary Research, 61, 1991.

Huybers, P. and Curry, W.: {L}inks between annual, {M}ilankovitch and continuum temperature variability, Nature, 441, 329–332, 2006.

Huybers, P. and Wunsch, C.: A depth-derived Pleistocene age model: Uncertainty estimates, sedimentation variability, and nonlinear climate change, Paleoceanography, 19, PA1028, 2004.

Jones, R. H.: {A}liasing with unequally spaced observations, Journal of Applied Meteorology, 11, 245–254, https://doi.org/10.1175/1520-0450(1972)011<0245:AWUSO>2.0.CO;2, 1972.

Kirchner, J. W.: Aliasing in 1/f(alpha) noise spectra: origins, consequences, and remedies., Physical review. E, Statistical, nonlinear, and soft matter physics, 71, 066 110, https://doi.org/10.1103/PhysRevE.71.066110, https://link.aps.org/doi/10.1103/PhysRevE.71.066110http://www.ncbi.nlm.nih.gov/pubmed/16089823, 2005.

MARGO Project Members: {C}onstraints on the magnitude and patterns of ocean cooling at the {L}ast {G}lacial {M}aximum, Nature Geoscience, 2, 127–132, 2009.

McGee, D., Winckler, G., Stuut, J. B. W., Bradtmiller, L. I., and Others: {T}he magnitude, timing and abruptness of changes in {N}orth {A}frican dust deposition over the last 20,000 yr, Earth and Planetary Science Letters, 371, 163–176, 2013.

Moore, M. I. and Thomson, P. J.: Impact of jittered sampling on conventional spectral estimates, Journal of Geophysical Research, 96, 18 519, https://doi.org/10.1029/91JC01623, 1991.

Pisias, N. G. and Mix, A. C.: {A}liasing of the geologic record and the search for long-period {M}ilankovitch cycles, Paleoceanography, 3, 613–619, 1988.

Rhines, A. and Huybers, P.: Estimation of spectral power laws in time uncertain series of data with application to the Greenland ice sheet project 2 δ¹⁸O record, Journal of Geophysical Research Atmospheres, 116, 1–9, https://doi.org/10.1029/2010JD014764, 2011.

Schulz, M. and Stattegger, K.: SPECTRUM: Spectral analysis of unevenly spaced paleoclimatic time series, Computers and Geosciences, 23, 929–945, https://doi.org/10.1016/S0098-3004(97)00087-3, 1997.

Shannon, C. E.: {C}ommunication in the presence of noise, Proceedings of the IRE, 37, 10–21, 1949.

Telford, R. J., Heegaard, E., and Birks, H. J. B.: The intercept is a poor estimate of a calibrated radiocarbon age, Holocene, 14, 296–298, https://doi.org/10.1191/0959683604hl707fa, 2004.

Tierney, J. E. and Tingley, M. P.: A Bayesian, spatially-varying calibration model for the TEX86proxy, Geochimica et Cosmochimica Acta, 127, 83–106, https://doi.org/10.1016/j.gca.2013.11.026, http://dx.doi.org/10.1016/j.gca.2013.11.026, 2014.

Van Sebille, E., Scussolini, P., Durgadoo, J. V., Peeters, F. J., Biastoch, A., Weijer, W., Turney, C., Paris, C. B., and Zahn, R.: Ocean currents generate large footprints in marine palaeoclimate proxies, Nature Communications, 6, 1–8, https://doi.org/10.1038/ncomms7521, http://dx.doi.org/10.1038/ncomms7521, 2015.

von Albedyll, L., Opel, T., Fritzsche, D., Merchel, S., Laepple, T., and Rugel, G.: 10 {B}e in the {A}kademii {N}auk ice core–first results for {CE} 1590–1950 and implications for future chronology validation, Journal of Glaciology, pp. 1–9, 2017.

Wunsch, C.: {T}he {N}orth {A}tlantic general circulation west of 50˜{W} determined by inverse methods, Reviews of Geophysics, 16, 583–620, 1978.

Wunsch, C.: 0n sharp spectral lines in the climate record and the millennial peak, Paleoceanography, 15, 417–424, 2000.

Wunsch, C.: {Greenland}–{A}ntarctic phase relations and millennial time-scale climate fluctuations in the {Greenland} ice-cores, Quaternary Science Reviews, 22, 1631–1646, 2003.

Wunsch, C. and Gunn, D. E.: {A} densely sampled core and climate variable aliasing, Geo-Marine Letters, 23, 64–71, 2003.

Zhao, N., Marchal, O., Keigwin, L., Amrhein, D., and Gebbie, G.: A Synthesis of Deglacial Deep-Sea Radiocarbon Records and Their (In)Consistency With Modern Ocean Ventilation, Paleoceanography and Paleoclimatology, 33, 128–151, 2018.